Fibers and Polymers (2024) 25:557–564
https://doi.org/10.1007/s12221-024-00468-w

Online ISSN 1875-0052
Print ISSN 1229-9197

REGULAR ARTICLE

Surface Modification and Antibacterial Functionalization of Polyester Fabrics Using Deep Eutectic Solvent and Its Composite Solution

Manman Zheng[1] · Yi Yang[1] · Haiwei Yang[1] · Hui Zhang[1] · Lele Zhang[1] · Weijie Zheng[1] · Zongqian Wang[1]

Received: 16 October 2023 / Revised: 21 December 2023 / Accepted: 30 December 2023 / Published online: 9 January 2024

Abstract

As an environmentally friendly solvent, deep eutectic solvent has become a research hotspot for fiber modification in recent years. In this paper, surface modification and functionalization of polyester fabrics (PET) were treated by the deep eutectic solvent of choline chloride/oxalic acid (ChCl/OA) and chitosan-dissolved ChCl/OA (ChCl/OA-CTS). The surface morphology, chemical structure, dimensional stability, mechanical properties, and antibacterial properties of PET before and after treatment were compared, and the results showed that PET fiber swelling occurred by ChCl/OA treatment, and fiber fineness increased by 15.92%. Scanning electron microscope (SEM) indicated that the surface roughness of the fiber increased and the surface etching occurred after washing and drying. Meanwhile, the adjacent fibers were "welded" to each other, resulting in increased friction between the fibers and improved stability of the fabric size. Fourier transform infrared (FTIR), energy dispersive spectrometers (EDS), and X-ray photoelectron spectroscopy (XPS) analysis showed that the chitosan was loaded on the surface of PET fiber after ChCl/OA-CTS treatment, the hydrophilicity of PET fiber was improved, and the inhibition rate of *Escherichia coli* (*E. coli*) and *Staphylococcus aureus* (*S. aureus*) was 92.04% and 92.16%, respectively. In conclusion, the PET was physically etched and reproduced, and the chitosan can be embedded in the fiber with the swelling of the fiber.

Keywords Deep eutectic solvent · PET · Chitosan · Surface modification · Antibacterial property

1 Introduction

As a novel green solvent, deep eutectic solvents (DES) have many unique chemical properties including low melting point, biodegradable, easy synthesis, chemical structure variability, and good solubility, which have been applied to the surface modification of materials, polyester degradation, extraction, separation, high-efficiency catalysis, and other fields [1–4]. In recent years, the application of DES in fiber modification has become a research focus. For example, Xu et al. [5] used choline chloride/oxalic (ChCl/OA) as the DES to etch the surface of cotton fabric, and the results showed that the reactivity of cotton fabric was increased, and hydrophobic samples were firmly grafted on the fabric surface to obtain the durable superhydrophobic cotton fabric. Wang et al. [6] used ChCl/OA to treat the surface of polylactic acid (PLA) fiber. Hydrogen bond receptors and donors of DES can interact with the active sites and chemical bonds on the molecular chain of PLA, which can result in the changes of chemical structure and microstructures and achieve the surface reengineering and control of hydrophilic and hydrophobic properties of PLA fiber. The experimental results showed that the roughness, reactivity, and hydrophily of the PLA surface were improved. Importantly, the excellent hydrophilicity of PLA fabrics can increase the adsorption and diffusion of dye molecules on the surface of the fiber, the original dyeing "boundary layer" was broken, and the dyeing energy resistance was reduced, showing an excellent dyeing performance in a low temperature.

Due to high crystallinity, strong mechanical properties, wear resistance, tensile resistance, and wrinkle resistance, Polyester (PET) is one of the most widely used and highest-yield synthetic fibers, and the production exceeds 80% of the total production of chemical fibers [7]. However, the disadvantages of chemical inertness, and low moisture regain result in the poor properties of hydrophilic, hygroscopic,

Manman Zheng and Yi Yang contributed equally to this work.

✉ Zongqian Wang
wzqian@ahpu.edu.cn

[1] Key Laboratory of Textile Fabric, School of Textiles and Garment, Anhui Polytechnic University, Wuhu, Anhui, China

antistatic, and dyeing, which influence comfort properties, and functional applications of PET textiles [8]. Hence, the development of PET modification technology is particularly important. Compared with conventional copolymerization and blending, surface modification of PET is a usual approach due to the advantages of simple process, and designability [9–12]. At present, The conventional surface modification methods of PET mainly include chemical modification [13], alkali reduction [14], finishing, and coating [15]. However, the use of large quantities of chemical reagents produces the generation of wastewater and breaks the strength and softness of fibers. Therefore, it is of great academic value to explore the green modification method of PET fiber, which meets the needs of industry development and creates significant economic and social benefits. The currently used green modification technologies include plasma modification [16] and radiation modification [17]. However, the above modification technologies must use special equipment and the modified fibers have poor durability. Therefore, it is urgent to develop novel green modification technologies for PET fibers.

DES modification is a new method for modifying the surface of PET. In our previous research [18], surface element distribution, group composition, and micro-morphology of PET fibers can be changed after DES modification. In addition, the surface roughness, hydrophilicity, and wicking ability of modified PET fibers can be increased. DES can quickly dissolve the disperse dye prepolymer to prepare high-efficiency and stable liquid disperse dyes to improve the dyeing quality of PET fabrics [19]. Nevertheless, the previous study primarily examined the alterations in an individual PET fiber and did not explore the impact of DES modification on the structure and interaction among neighboring PET fibers. Moreover, the surface functional modification of PET fiber by DES was also not studied. Therefore, in this paper, the PET fiber was modified by the deep eutectic solvent of choline chloride/oxalic acid (ChCl/OA) and chitosan-dissolved ChCl/OA (ChCl/OA-CTS). Microstructure, chemical structure, dimensional stability, mechanical properties, and antibacterial properties of PET fibers were studied, and the internal action mechanism of DES on PET fiber was also expounded. The antibacterial mechanism of PET fibers after modification of ChCl/OA-CTS was investigated.

2 Experimental Section

2.1 Chemicals and Materials

PET (78 g/m^2, $M_w = 40{,}000$) was purchased from Xinfeng Printing and Dyeing Co., Ltd. (Huzhou, China). Coline chloride (ChCl), oxalic acid (OA), sodium hydroxide (NaOH), sodium chloride (NaCl), and chitosan (degree of deacetylation $\geq 95\%$, $M_w = 10$ kDa) were obtained from Sinopharm Chemical Reagent Co., Ltd. (Shanghai, China). Peptone, yeast powder, and nutrient agar medium were purchased by Hangzhou Gaojing Fine Chemical Co., Ltd. (Hangzhou, China).

2.2 Preparation of ChCl/OA and ChCl/OA-CTS

A mixture of chloride (ChCl) and ethylene glycol (EG), urea (Ur), or oxalic acid (OA) with a certain mass ratio was added to a three-mouth flask with a rubber stopper. Subsequently, the mixture was stirred and heated at 100 °C until the solid was dissolved and became a clear and transparent liquid. Finally, the mixed solvent was stirred for another 1 h and the deep eutectic solvents of chloride/ethylene glycol (ChCl/EG), chloride/urea (ChCl/Ur), and choline chloride/oxalic acid (ChCl/OA) were obtained, respectively. The different acid-alkalinity and mass ratios of DES were optimized. As shown in Fig. S1a, the contact angles (CA) of PET fibers fell from 141.86° to 115.54° after ChCl/OA treatment, while the CAs of ChCl/EG and ChCl/Ur-treated PET fibers were 130.69° and 127.99°. Furthermore, the mass ratio of ChCl and OA was also optimized (Fig. S1b). It can be seen that CAs of ChCl/OA-treated PET declined and reached a minimum value (115.54°) at a mass ratio of ChCl and OA was 1:3 (Fig. S2). As shown in Fig. S2, ChCl/OA exhibited colorless and transparent.

Chitosan (0.5 g) was dissolved by ChCl/OA (50 mL), and chitosan-dissolved ChCl/OA (ChCl/OA-CTS) was obtained.

2.3 Modification of PET

PET was immersed in ChCl/OA with a mass ratio of 30:1 at 90 °C for 30 min [20]. Subsequently, the PET was washed with deionized water to remove the residual ChCl/OA and dried at 70 °C. Finally, the modified PET fiber was obtained (W-PET).

As shown in Fig. 1, the PET fiber was immersed in ChCl/OA-CTS (1 wt%) under the same conditions as W-PET [21, 22], and the obtained sample was marked CTS-PET.

2.4 Characterization

The surface morphologies of PET, W-PET, and CTS-PET were observed by scanning electron microscope (SEM, S-4800, Hitachi, Japan) with a 2.0×10^3 magnification at an accelerating voltage of 5.0 kV. Before the SEM–EDX test, the surface of the sample was treated with the gold deposit in a vacuum for 1 min. The SEM with energy dispersive X-ray spectrometry (EDS) was used to perform surface elemental mapping and determine the surface elemental composition of CTS-PET. PET and CTS-PET were washed with ethanol and the functional groups were characterized by a Fourier

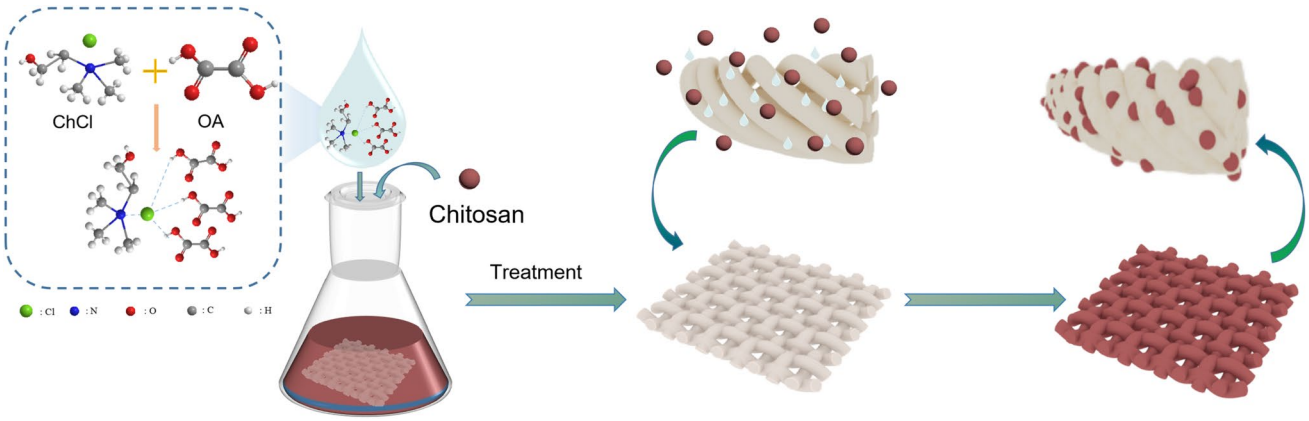

Fig. 1 Preparation process of CTS-PET

transform infrared spectrometer (FT-IR) with an ATR module (Prestige-21, Shimadzu, Japan). The transmittance of the infrared in individual samples of the substrate was recorded from 4000.0 to 600.0 cm^{-1} at a resolution of 2.0 cm^{-1} for infrared spectra. The crystalline structures of prepared PET and W-PET fibers were analyzed by X-ray diffraction (XRD, D8, Bruker, Germany) equipped with Cu K radiation (40 kV and 200 mA) in a 2θ between 5° and 65°. X-ray photoelectron spectroscopy (XPS) was used to identify elements, and chemical valence states of PET and CTS-PET in a system equipped with a Thermo Scientific K-Alpha electron analyzer (Kratos Co., UK). XPS was performed with 1486.6 eV Al Kα excitation radiation, operated at 12 kV and 15 mA. And the C1S line at 284.6 eV was set to the binding energies. The breaking strength of PET and W-PET fibers was tested by an electronic fabric strength tester (YG (B) 026G, Darong Textile Co., Ltd, China) according to the standard: GBT 3923.1-2013, and each group of samples was measured three times to obtain the average value. The contact angle (CA) of static water droplets (5 μL) was measured using the contact angle meter equipped with a CCD camera (OSA-60, LAUDA, Germany), and each group of samples was measured three times to obtain the average value. According to the previous related research, the antimicrobial properties of PET and CTS-PET fibers were compared [23]. Specifically, *Escherichia coli* (ATCC 43895) and *Staphylococcus aureus* (ATCC 6538) were added to the saline solution (4 mL) at the vortex for 10 s to mix well. Subsequently, the above bacterial solution was diluted 10,000 times, and the above-diluted bacteria solution (0.02 mL) was added to the surface of the samples and maintained for 1 h. Finally, the sample was added to the saline solution (5 mL) and dispersed by the vortex for 10 s. 0.1 mL dispersed bacterial culture medium was coated on the surface of the solid medium at 37 °C for 24 h. The clump counts were counted, and each group of samples was measured three times to obtain the average value.

The weight loss ratio of W-PET was calculated by Eq. (1).

$$wl\ (\%) = \frac{m_0 - m_1}{m_0} \times 100\% \tag{1}$$

where the wl is the weight loss ratio of W-PET, m_0 is the weight of PET fibers, and the m_1 is the weight of W-PET.

PET and W-PET were dried at 50 °C after ultrasonic treatment for 60 min. The area loss rates of samples were calculated by Eq. (2).

$$sl(\%) = \frac{s_0 - s_1}{s_0} \times 100\% \tag{2}$$

where the sl is the area loss rates, s_0 is the area fabric without ultrasonic treatment, and s_1 is the area fabric after ultrasonic treatment.

3 Results and Discussions

3.1 Preparation and Characterization of PET and W-PET

After modification of ChCl/OA, the surface morphologies and crystalline state PET fibers were studied. As seen in Fig. 2a, b, the surface of the PET fiber was smooth and had a about diameter of 8.99 μm. The surface of W-PET was etched and surface roughness increased. Meanwhile, the diameter of W-PET (11.13 μm, Fig. 2c, d) increased by about 23.80% as compared with PET, showing a similar swelling effect to that of traditional chemical agents with a high temperature (140 °C) [24]. It is attributed that the ChCl/OA can cause the fiber to swell, enhance the molecular chain mobility, and produce a larger free volume. The change of crystalline structures of PET and W-PET were verified by XRD analysis. As shown in Fig. 3, the XRD spectrum of PET exhibited characteristic peaks at 2θ = 16.4°, 22.7°, and 25.2°, corresponding to the (010), (110), and (100) crystallographic planes [18], respectively. Compared with PET, the

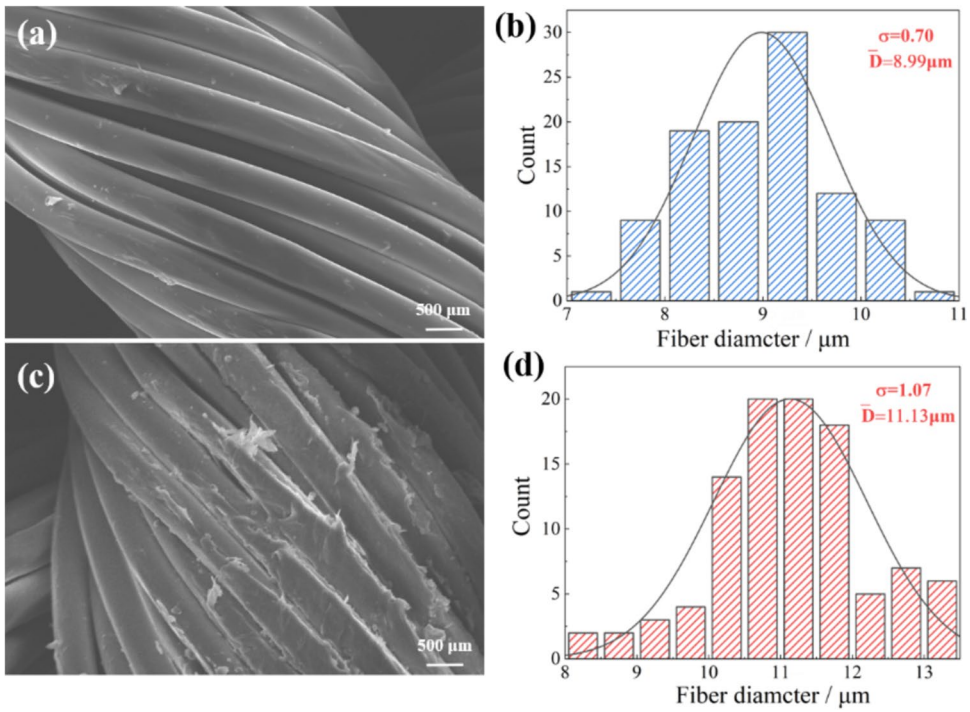

Fig. 2 SEM images of **a** PET, **c** W-PET fibers, diameter distribution of **b** PET, and **d** W-PET

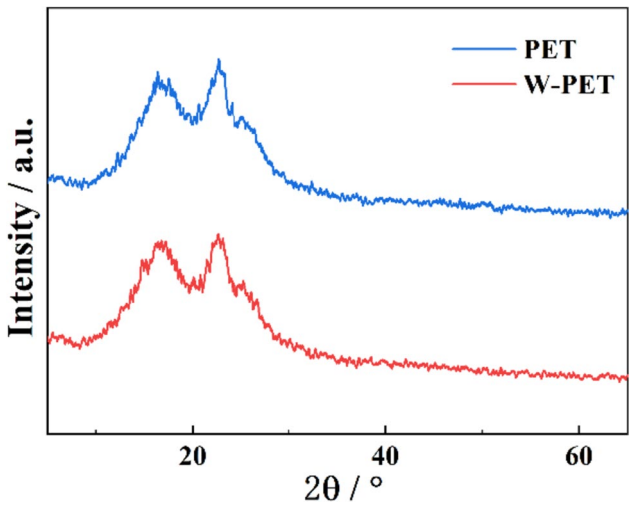

Fig. 3 XRD curves of PET, and W-PET fibers

characteristic peaks of W-PET were similar to PET, indicating that the original crystalline structures of PET not be destroyed.

After ultrasonic treatment, the dimensional stability of PET and W-PET was studied and the result was shown in Fig. 4a, b. In Fig. 4a, PET appeared to slip, fall off, and deformation under the mechanical effects and sound cavitation of ultrasound. Meanwhile, the area loss of PET reached (43.72 ± 0.76) %, while W-PET was not affected by ultrasonic waves, exhibiting excellent dimensional stability. SEM images (Fig. 4c) of W-PET were used to explain the excellent dimensional stability of W-PET. As shown in Fig. 4c, the surface of PET was smooth and had large spaces between the fibers, while the surface of W-PET was etched and a large number of "welding points" between the fibers appeared, preventing the slip, fall off, deformation of W-PET. This phenomenon can be attributed to the neighboring fibers of PET were swelled in the process of ChCl/OA treatment, and the surface of PET fibers was reconstructed after moving to the water phase, and the adhesion between fibers occurred. Compared with traditional thermal bonding [25], coating [26], chemical [27], and other methods, DES-treated fibers exhibited better dimensional stability and had a green, efficient convenient processing.

Mechanical properties are the key indexes to evaluate the performance of textiles. In this paper, the mechanical properties of PET and W-PET were compared in Fig. 4d. The breaking force of PET was (448.6 ± 9.98) N, while the breaking force of W-PET increased to (521.4 ± 7.20) N. Meanwhile, elongation at break of W-PET also increased by (27.25 ± 1.04) %. The above results indicated that the resilience of W-PET was better than PET. This is attributed to the fact that the adhesion between the fibers can increase the force of friction to improve the mechanical properties of W-PET.

3.2 Characterization of CTS-PET

Functional groups of PET, W-PET, and CTS-PET were characterized by FT-IR-ATR, and the results were shown in Fig. 5a. The absorption peaks at 3030 and 2860 cm^{-1}, were

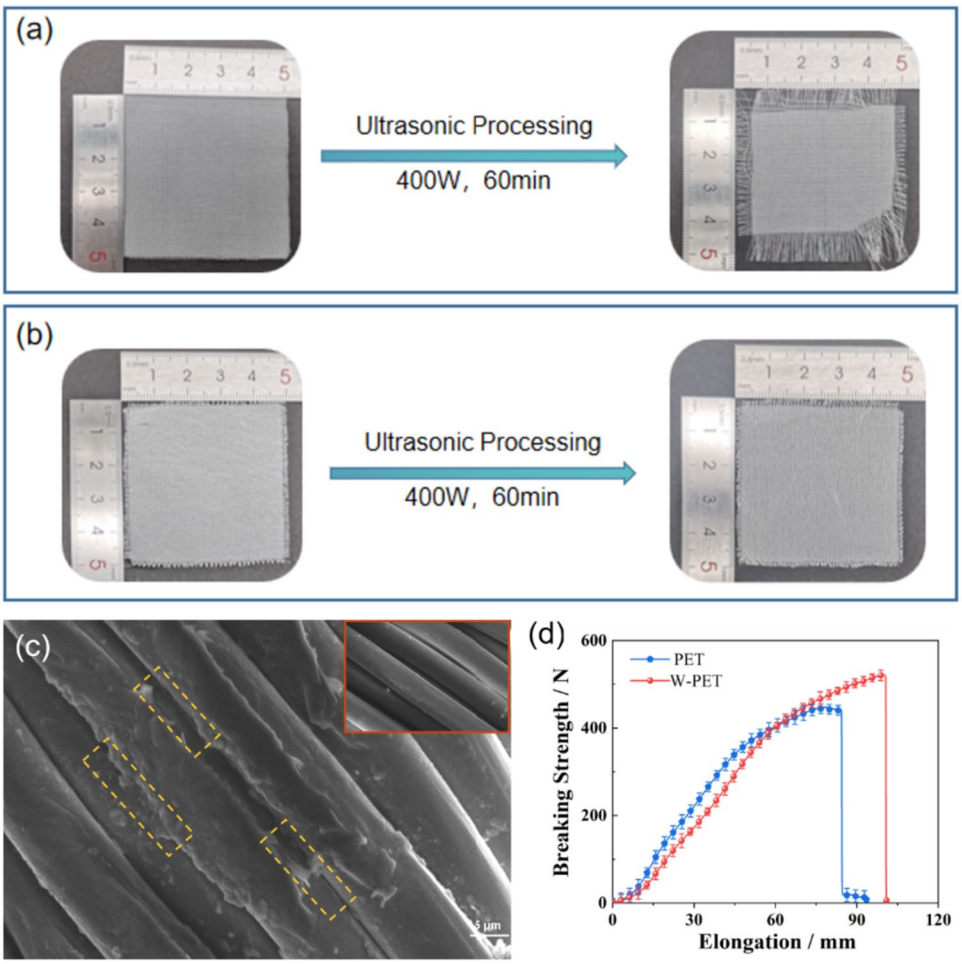

Fig. 4 Photos of ultrasonic treated **a** PET and **b** W-PET, **c** SEM images of W-PET, and the **d** curves of elongation at break of PET and W-PET

assigned to stretching vibration absorption peaks of C–H on the benzene ring. The peaks at 1712 and 1242 cm^{-1} were assigned to the stretching vibration of C=O, and –COO–, respectively. Besides, an obvious stretching vibration absorption at the peak of 722 cm^{-1} was assigned to the substituent on the benzene ring [28, 29]. Compared with PET, no new absorption peaks appeared in W-PET, indicating the chemical structure of the PET surface did not change after modification of ChCl/OA. Furthermore, in the FT-IR of CTS-PET, an absorption peak at 3430 cm^{-1} was assigned to stretching vibration absorption peaks of NH_2 [29, 30], indicating that PET had been successfully modified by ChCl/OA-CTS. The EDS analyses of CTS-PET were shown in Fig. 5b. It can be seen that the element of N was observed, which was attributed to the introduction of chitosan. XPS spectra of PET and CTS-PET were shown in Fig. 5c–e. It can be clearly seen that a new peak of CTS-PET located at 400 eV can be assigned to the nitrogen element (N) as compared with PET in Fig. 5c [31]. By peak-differentiating and imitating, C 1s peak of PET could be fitted to three lines shapes with the binding energy at 283.88, 285.58, and 287.78 eV, which exhibited the presence of C*–C, C*–O, and C*=O. Compared with PET, C 1s spectra of CTS-PET can be deconvoluted into four distinct peaks at 283.88, 285.58, 287.78, and 287.58 eV. Importantly, the peak at 287.58 eV was attributed to C–N [30], which indicated that PET had been successfully modified by ChCl/OA-CTS.

3.3 The Hydrophilic and Antibacterial Properties of CTS-PET

In general, PET and its textiles are prone to hydrophobic fabrics because they have a large number of ester groups in their structure. In Fig. 6, the wettability of the PET fabrics and CTS-PET fabrics was studied by measuring the static water contact angle (CA). Compared with PET, the CA of CTS-PET was 0°, exhibiting excellent hydrophilicity. This phenomenon can be explained that chitosan contains a large number of hydrophilic functional groups (hydroxyl and amino), resulting in a hydrophilic surface of CTS-PET after modification of chitosan.

The antimicrobial properties of PET fabrics modified with chitosan were tested using the oscillation method (GB/T20944.3-2008). The growth of *S. aureus* and *E. coli* was shown in Fig. 7. A large number of bacteria were grown in the Petri dishes of the PET fabrics (Fig. 7a, c), indicating

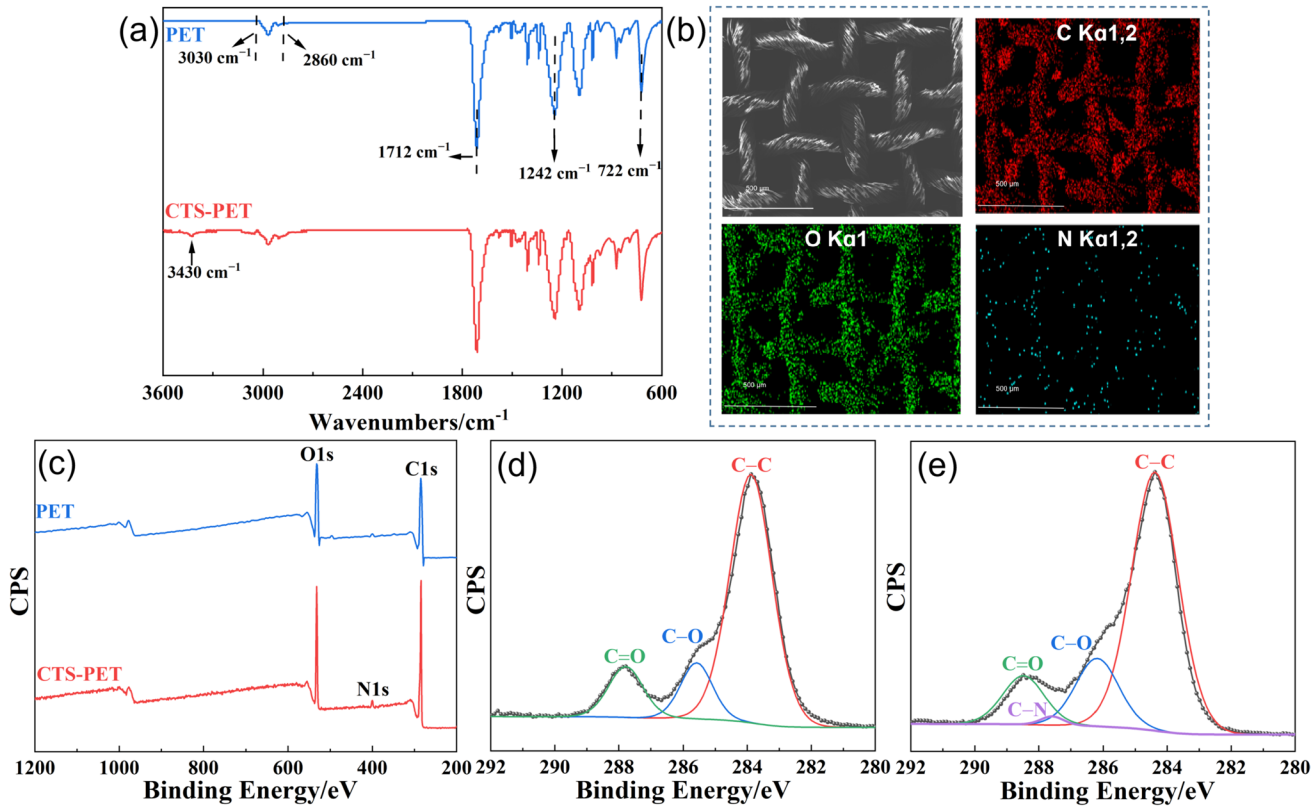

Fig. 5 **a** FT-IR spectra of PET, and CTS-PET, **b** EDS spectra of CTS-PET, and **c** XPS over spectra of PET, CTS-PET, **d** C 1s spectra of PET, and **e** C 1s spectra of CTS-PET

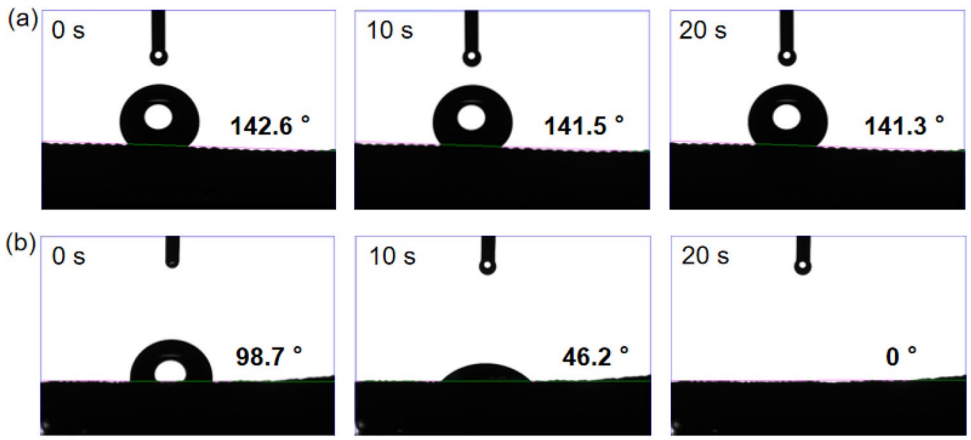

Fig. 6 The contact angle of **a** PET, and **b** CTS-PET

the lack of antibacterial effect of these fabrics on *E. coli* and *S. aureus*. The CTS-PET fabrics showed some degree of bacterial reduction against *E. coli* and *S. aureus*; the antibacterial rate was 92.16% for *S. aureus* and 92.04% for *E. coli*. Surface grafting [32], coating [33, 34], and other forms of chemical modification [22] were often applied to the antibacterial modification of polyester fabrics. However, the above chemical modification had the disadvantages of poor chemical stability, low durability, poor washing fastness, environmental pollution, and poor antibacterial properties. The chitosan-treated PET fabrics had better antibacterial properties. Since the chitosan treatment changed the surface of the fabrics, the physical absorption of the CTS-PET on the surface of the fabrics increased. Chitosan on the surface of CTS-PET played a vital role in the antibacterial activity, because the amino group of chitosan adsorbs H^+ to form NH_3^+ under acidic conditions and adsorbs the negatively charged microbial cell wall, causing the cell wall to dissolve

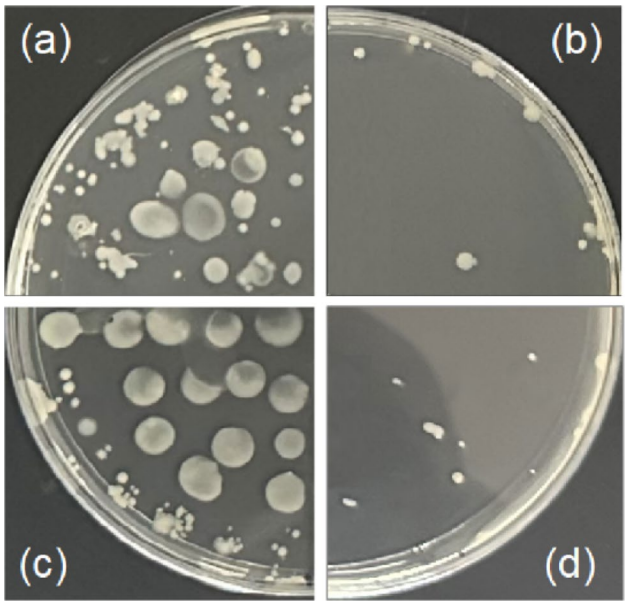

Fig. 7 Antibacterial properties of the (**a** *E. coli*, **c** *S. aureus*) PET, and (**b** *E. coli*, **d** *S. aureus*) CTS-PET fabrics

and rupture [35]. More importantly, the antibacterial modification method described in this paper is green and effective, making up for the shortcomings of the above chemical modification.

3.4 Preparation Mechanism of CTS-PET

In this paper, PET was high-efficiency modified by ChCl/OA-CTS, which can reduce the use of chemicals and achieve energy conservation and emission reduction. The preparation mechanism of CTS-PET was studied (Fig. 8).

As shown in Fig. 8, strong hydrogen bonding forces of ChCl/OA-CTS can effectively attack the ester-based carbon in PET fibers, resulting in cleavage of fiber macromolecules, and swelling of fibers. Afterward, chitosan effectively enters the amorphous region of PET fibers while filling the junctions and etching points embedded between fibers, endowing better antibacterial and hydrophilic properties. Finally, surface reconstruction between CTS-PET fibers was realized in the water phase, the chitosan was closed to the surface of the CTS-PET, and the CTS-PET fibers were tightly bonded, leading to a better washing fastness of CTS-PET.

4 Conclusions

The objective of this study was to develop functionalized PET fibers with improved antibacterial and hydrophilic properties using a compound solution of ChCl/OA-CTS. The experiment results showed that the surface roughness of PET increased, PET fibers swelled and the diameter increased by 15.92%, the adhesion between the PET fibers appeared on

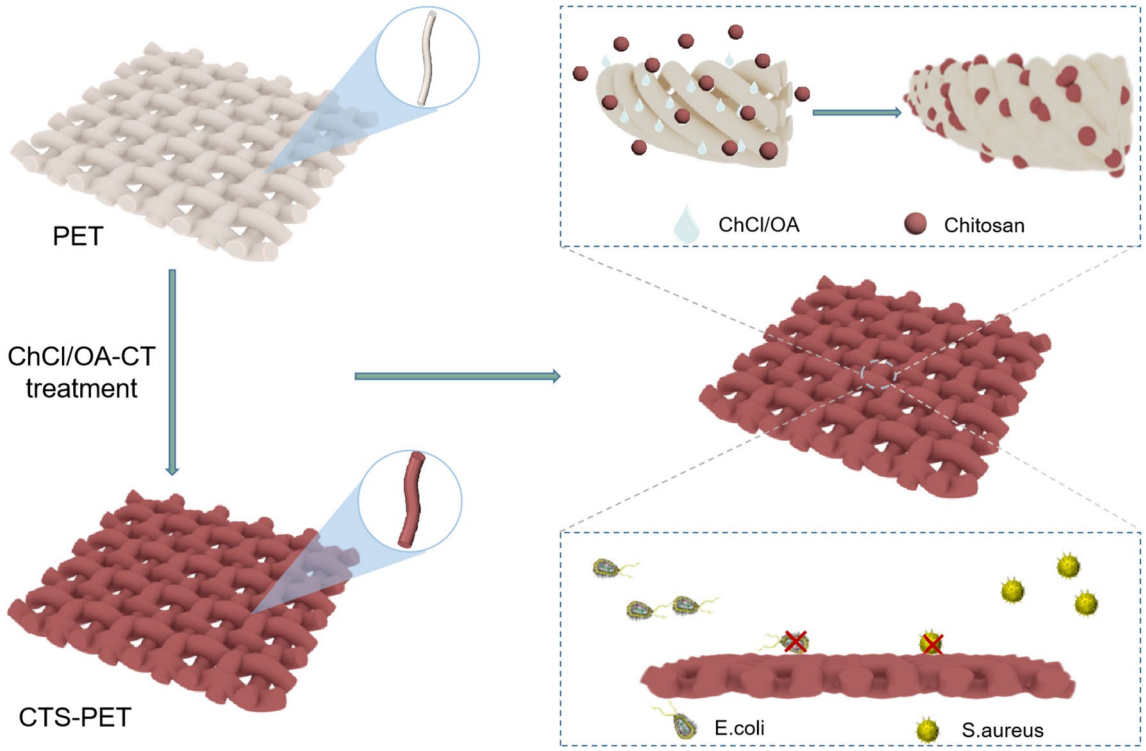

Fig. 8 Preparation mechanism of CTS-PET

the PET surface, and the dimensional stability of the PET fabrics was improved. FT-IR, EDS, and XPS indicated that chitosan was successfully grafted on the surface of CTS-PET. The CA of CTS-PET decreased from 142.3° to 0°, and the inhibition rates of *E. coli* and *S. aureus* were 92.04% and 92.16%, respectively. This work provides a simple, efficient, and green strategy for the modification of textiles.

Supplementary Information The online version contains supplementary material available at https://doi.org/10.1007/s12221-024-00468-w.

Acknowledgements This work was supported by the Key Research and Development Plan Project of Anhui Province [Grant numbers: 2023t07020001, 2022a0502029]; Anhui Natural Science Foundation [Grant numbers: 2308085ME144]; National Advanced Printing and Dyeing Technology Innovation Center Research Project [Grant numbers: 2022GCJJ13]; The University Synergy Innovation Program of Anhui Province (GXXT-2023-035); Key Research and Development Plan Project of Wuhu city (2023yf002, 2022jc18, 2022yf14); National College Student Innovation and Entrepreneurship Training Program (202210363002); Schoollevel scientific research project of Anhui Polytechnic University (KZ42020108); Starting Research Fund of Anhui Polytechnic University [Grant numbers: 2022YQQ012]; Research Fund of Anhui Polytechnic University [Grant numbers: Xjky2022071]; Opening Fund of Zhejiang Provincial Key Laboratory of Clean dyeing and finishing Technology [Grant numbers: QJRZ2302].

Author Contributions MZ: conceptualization, methodology, investigation, writing-original draft. YY: conceptualization, methodology, investigation, writing-original draft. HY: conceptualization, methodology, investigation. HZ: conceptualization, methodology, investigation. LZ: conceptualization, methodology, investigation. WZ: conceptualization, methodology, investigation. ZW: supervision, validation, writing-review and editing, funding acquisition.

Data Availability The datasets used and/or analyzed during the current study are available from the corresponding author (Zongqian Wang) on reasonable request.

Declarations

Conflict of Interest The authors declare that they have no conflict of interest.

References

1. L.I.N. Tome, V. Baiao, W. da Silva, C.M.A. Brett, Appl. Mater. Today **10**, 30 (2018)
2. B.B. Hansen, S. Spittle, B. Chen, D. Poe, Y. Zhang, J.M. Klein, A. Horton, L. Adhikari, T. Zelovich, B.W. Doherty, B. Gurkan, E.J. Maginn, A. Ragauskas, M. Dadmun, T.A. Zawodzinski, G.A. Baker, M.E. Tuckerman, R.F. Savinell, J.R. Sangoro, Chem. Rev. **121**, 1232 (2021)
3. B.L. Chen, Z.Q. Peng, C. Li, Y.C. Feng, Y. Sun, X. Tang, X.H. Zeng, L. Lin, Chemsuschem **14**, 1496 (2021)
4. J.X. Wu, Q.H. Liang, X.L. Yu, Q.F. Lu, L.B. Ma, X.Y. Qin, G.H. Chen, B.H. Li, Adv. Func. Mater. **31**, 25 (2021)
5. Q.B. Xu, X.Y. Wang, P. Wang, L.Z. Cheng, Y.P. Wan, Z.Q. Wang, Mater. Today Chem. **26**, 12 (2022)
6. L.L. Ying, H.T. Zhao, C.L. Li, H.W. Yang, C.G. Hu, Z.Q. Wang, Macromolecules **55**, 6238 (2022)
7. G. Dalla Fontana, R. Mossotti, A. Montarsolo, Environ. Pollut.Pollut. **264**, 6 (2020)
8. C.L. Zuo, Y.S. Liu, Y.B. Guo, W. Tan, Y.L. Ren, X.H. Liu, Polym. Degrad. Stab.. Degrad. Stab. **209**, 13 (2023)
9. X. Dong, R.T. Duan, Y.P. Ni, Z.J. Cao, L. Chen, Y.Z. Wang, Polym. Degrad. Stab.. Degrad. Stab. **146**, 105 (2017)
10. P.T. Fang, X.M. Lu, Q. Zhou, D.X. Yan, J.Y. Xin, J.L. Xu, C.Y. Shi, Y.Q. Zhou, S.Q. Xia, Chem. Eng. J. **451**, 15 (2023)
11. N. Poulopoulou, N. Kasmi, M. Siampani, Z.N. Terzopoulou, D.N. Bikiaris, D.S. Achilias, D.G. Papageorgiou, G.Z. Papageorgiou, Polymers **11**, 15 (2019)
12. L. Chen, Y. Guo, T. Fu, H.B. Zhao, X.L. Wang, Y.Z. Wang, Macromolecules **54**, 4412 (2021)
13. T. Harifi, M. Montazer, Ultrason. Sonochem.. Sonochem. **37**, 158 (2017)
14. S. Lee, RSC Adv. **12**, 22911 (2022)
15. Q. Kong, Z.G. Li, Z.L. Zhang, X.H. Ren, J. Ind. Eng. Chem. **83**, 430 (2020)
16. J.C. Lv, Q.Q. Zhou, T. Zhi, D.W. Gao, C.X. Wang, J. Clean. Prod. **118**, 187 (2016)
17. M. Jamalzadeh, M.J. Sobkowicz, Polym. Degrad. Stab.. Degrad. Stab. **206**, 11 (2022)
18. Y.Y. Zhang, L.L. Ying, Z.Q. Wang, Y. Wang, Q.B. Xu, C.L. Li, Polymer **234**, 8 (2021)
19. M.M. Zheng, Y. Sun, C.L. Li, Y.H. Lu, Y.Q. Dai, Z.Q. Wang, Coloration Technol. **13** (2023). https://doi.org/10.1111/cote.12673
20. Y. Zhang, L. Ying, Z. Wang, Y. Wang, Q. Xu, C. Li, Polymer **234**, 124246 (2021)
21. Z. Sun, Y. Yue, W. He, F. Jiang, C.-H. Lin, D.Y.H. Pui, Y. Liang, J. Wang, Build. Environ. **180**, 107020 (2020)
22. J. Tan, H. Deng, F. Lu, W. Chen, X. Su, H. Wang, Polymers **15**, 4376 (2023)
23. Y.P. Wang, Z.Q. Wang, Y.F. Wang, H.W. Yang, K.M. Wu, W. Wei, J. Textile Res. **44**, 149 (2023)
24. J.P. Wang, W.Q. Cheng, Y.Y. Gao, L. Zhu, L.J. Pei, Polymers **11**, 520 (2019)
25. Y.C. Chuang, L. Bao, M.C. Lin, T.A. Lin, C.W. Lou, Polymers **11**, 706 (2019)
26. J. Nasser, K. Steinke, L.A. Groo, H.A. Sodano, Adv. Mater. Interfaces (2019). https://doi.org/10.1002/admi.201900881
27. H.-Y. Zhao, Y.-Q. Qiang, H.-K. Peng, M.-F. Xing, X.-Y. Zhang, C.-W. Lou, Fibers Polym. **22**, 3309 (2021)
28. S. Klebert, S. Tilajka, L. Romanszki, M. Mohai, E. Csiszar, Z. Karoly, Surf. Interfaces **22**, 10 (2021)
29. M. Masoomi, M. Tavangar, S.M.R. Razavi, RSC Adv. **5**, 79200 (2015)
30. L.F. Zemljic, T. Tkavc, A. Vesel, O. Sauperl, Appl. Surf. Sci. **265**, 697 (2013)
31. N. Behary, A. Perwuelz, C. Campagne, D. Lecouturier, P. Dhulster, A.S. Mamede, Colloids Surf. B BiointerfacesBiointerfaces **90**, 137 (2012)
32. G. Zhang, D. Wang, Y. Xiao, J. Dai, W. Zhang, Y. Zhang, Nanotechnol. Rev.. Rev. **8**, 100 (2019)
33. J. Feng, S. Xu, G. Pan, L. Yao, Y. Guan, L. Zhou, L. Cui, Z. Yang, Nanotechnol. Rev.. Rev. **10**, 1740 (2021)
34. Z.A. Raza, F. Anwar, S. Abid, Polym. Bull.. Bull. **76**, 3039 (2019)
35. Z.B. Zhang, Z.Y. Zhao, Z.Z. Zheng, S. Liu, S.X. Mao, X.X. Li, Y.S. Chen, Q.S. Mao, L. Wang, F.J. Wang, X.Q. Wang, Z.J. Pan, G. Li, Appl. Surf. Sci. **495**, 10 (2019)